A 2×2 Split Cross-Bar Optical Switch Using a Hybrid Actuation Configuration

Bo-Ting Liao, Bonnie Tingting Chia, Sun-Chih Shih, Kuang-Chao Fan, and Yao-Joe Joseph Yang, *Member, IEEE*

***Abstract*—In this paper, a 2×2 split cross-bar optical switch which employs a hybrid actuation configuration is presented. The main advantages of this proposed switch include low actuation voltage, low power consumption, and easy fiber alignment. This optical switch consists of a micromachined micro-mirror structure and a mini-actuator module. The micro-mirror structure, which comprises two movable vertical mirrors with cantilevers, two fixed vertical mirrors, and light-path trenches, is realized by using a simple KOH silicon etching process. The mini-actuator module, which includes two commercially-available electromagnetic bistable actuators attached with L-shaped arms, is used to actuate micro-mirrors. The measured insertion losses of the proposed switch is between -1– $-$ 1.2 dB, the cross-talk is about -60 dB, and the switching time is less than 13 ms. The long-term reliability test of the SCB switch is performed by continuously actuating the device for 10 000 cycles at 1 Hz, and the deviation of the measured insertion loss is less than 0.05 dB.**

***Index Terms*—Bi-stable actuator, micro-electro-mechanical systems, micro-mirror, optical communication, optical switch.**

I. Introduction

OPTICAL switches are widely used for many modern fiber-optic network applications, such as network protection, wavelength routing, network management, and so on [1]. All-optical switches, which enable signals to be switched in optical domain without the need of optical-electrical-optical (OEO) conversions, are capable of reducing the network complexity, power consumption and system size [2]. Therefore, the development of all-optical switches has drawn attention in the telecommunication industries.

Many designs of micromachined all-optical switches [3]–[6] have been proposed in recent years. In general, micromachined optical switches can be classified into the three-dimensional (3-D) type [7]–[10] and the two-dimensional (2-D) type [11]–[17]. The 3D-type switches, which tilt micromirrors to route optical signals, usually need precise control of mirror positions. Unlike 3-D switches, the mirror of a 2D-type switch is usually actuated in "binary" form (i.e., two states). Therefore, the driving mechanism for 2-D devices is relatively simple. Besides, 2-D switches possess advantages of low cost and easy fabrication process when compared with 3-D switches. These advantages make the 2-D switches more suitable for low-port-count applications, such as 1×2 or 2×2 switches.

For 2D-type devices, there are two conventional designs of 2×2 optical switches: the *cross-bar design* [11]–[14] and the *mirror-array design* [15], [16]. In the *cross-bar design*, four fiber channels are arranged in a *cross* configuration. A tiny mirror slides in and out of the intersection point of the light paths, so the light beams of the input channels either cross to the fibers of the output channels on the opposite side, or are reflected to the other output channels. However, the mirror employed in a cross-bar switch must be double-sided. Also, the mirror side-length should be greater than 500 μm for fully reflecting the light beams from collimators. In addition, the thickness of the double-sided mirror must be very thin (e.g., less than 2 μm) for minimizing optical misalignment caused by mirror thickness. Therefore, these constraints on mirror dimensions increase the complexity of fabrication. As for the *mirror-array design*, four mirrors are arranged in a 2×2 array. Each mirror, which is located at the crossing position of an input and an output channel, reflects the light beam to the desired output channel. Although this type of design does not have the aforementioned misalignment issue caused by mirror thickness, it requires four movable mirrors and four actuators for switching. Therefore, the *split cross-bar* (SCB) design, which possesses the advantages over the cross-bar and mirror-array designs, had been proposed in [18], [19]. More details of the SCB design will be described in next section. The major advantages of the SCB devices include: (1) thin vertical mirrors are not required, and (2) only two movable mirrors and two actuators are needed for operation.

In this work, we propose a novel approach to realize a SCB 2×2 optical switch by utilizing a simple micromachining process and a hybrid actuation method. The device consists of a micromachined mirror array and an actuation module. A *single-step* anisotropic silicon etching process, which is quite simple and low cost, is employed to fabricate the mirror array. This process can monolithically create micro-mirror structures which include vertical mirrors and cantilevers [11]. Also, the fabricated vertical mirrors are self-aligned to the etched light-path trenches for easy fiber alignment. As for the actuation module, two electromagnetic mini-actuators attached with L-shaped arms are employed for bistable mirror switching. This proposed actuation module requires a very simple driving circuit, and can be easily integrated with the mirror array.

This paper is organized as follows: the device designs are described in Section II. In Section III, we will present the fabrication process. The measurements of the SCB switch are illustrated in Section IV. The conclusion of this paper is presented in Section V.

Manuscript received April 16, 2010; revised August 04, 2010; accepted August 13, 2010. Date of publication August 30, 2010; date of current version September 24, 2010. This work was supported in part by the National Science Council, Taiwan, under Contract NSC 97-2221-E-002-063.

The authors are with the Department of Mechanical Engineering, National Taiwan University, Taipei, 106, Taiwan (e-mail: yjy@ntu.edu.tw).

Color versions of one or more of the figures in this paper are available online at http://ieeexplore.ieee.org.

Digital Object Identifier 10.1109/JLT.2010.2070834

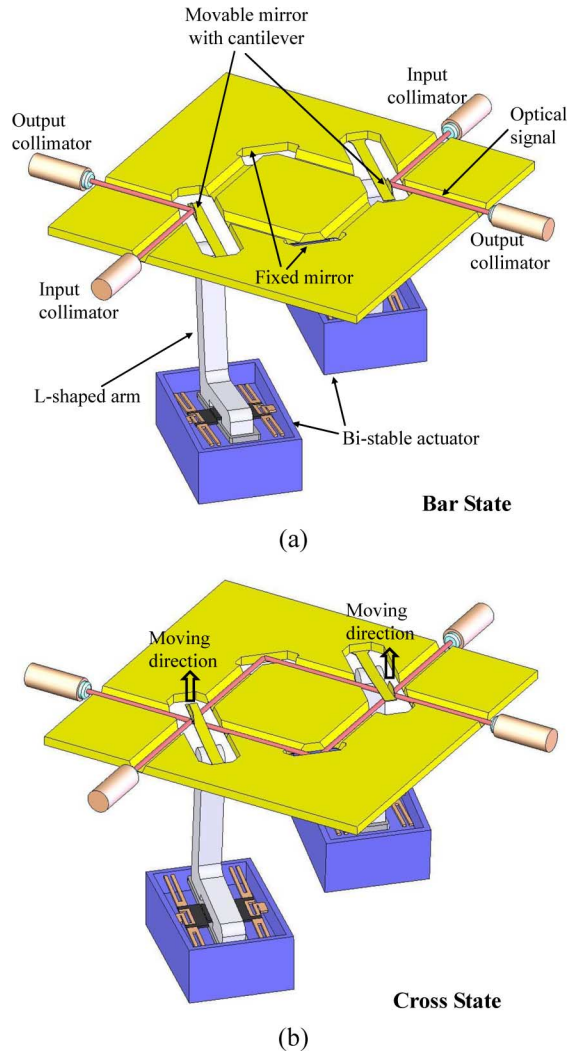

Fig. 1. The operational principle of the SCB switch. (a) The bar state: the L-shaped arm does not contact the cantilever so that the movable mirrors are in the light path and precisely redirect optical signals to the desired output channels. (b) The cross state: the cantilevers are pushed up by the L-shaped arm and the movable mirrors are out of the light path. Optical signals are reflected by the fixed mirrors.

II. Design and Configuration

Fig. 1 illustrates the operational principle of the proposed SCB switch. The switch is composed of a monolithically micromachined silicon micro-mirror structure and a mini-actuator module. The silicon micro-mirror structure includes two movable mirrors, two fixed mirrors, two cantilevers, and light-path trenches. The mini-actuator module consists of two commercially-available electromagnetic bistable actuators (TQ2-L2-5V, Panasonic) attached with L-shaped arms. Each mini-actuator can retain the mirror at either one of the two stable positions without consuming any electrical power. When the L-shaped arms do not contact the cantilevers of the two movable mirrors, the mirrors are located inside the light path and precisely redirect optical signals to the output channels (the bar state, as shown in Fig. 1(a)). When the cantilevers are pushed up by the L-shaped arms, the optical signals pass under the mirrors and then are reflected to other output channels by the fixed mirrors (the cross state, as shown in Fig. 1(b)). In addition, this hybrid integration of the mirror array and the actuation module can effectively eliminate the process difficulty of monolithically integrating microactuators on the mirror array. Also, one important advantage of this design has to be emphasized: the optical signals are reflected by the mirrors only when the cantilevers do not contact actuators (i.e., the cantilevers are under zero external force). Since the single-crystal mirror structures are stress free at this state, the positions of the mirrors are well-aligned, and can reflect light beam precisely.

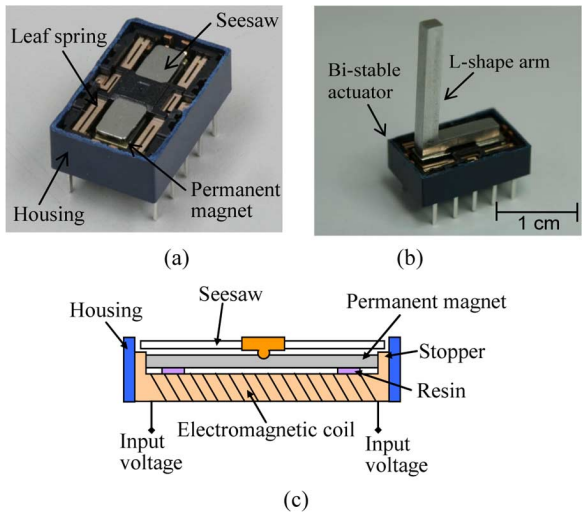

Fig. 2. (a) The picture of the commercially-available electromagnetic bistable actuator. (b) The picture of the mini-actuator, including L-shaped arm and bistable actuator. (c) Cross-sectional schematic drawing of the bistable actuator.

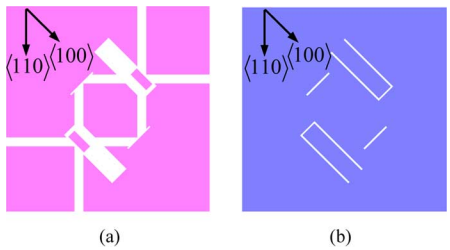

Fig. 3. (a) Mask layout of the movable mirrors, the fixed mirrors, and light-path trenches for the SCB switch device. (b) Backside mask layout of the cantilevers and the fixed mirrors.

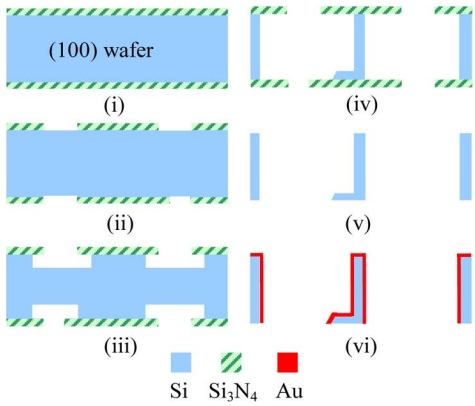

Fig. 4. The fabrication process of the silicon micro-mirror structure.

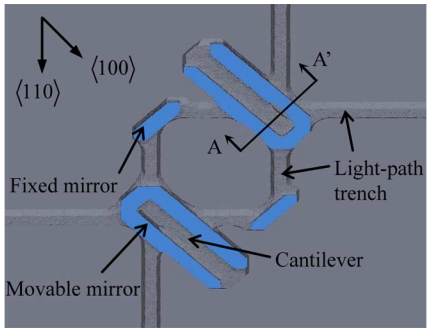

Fig. 5. The simulated results of the KOH etching process.

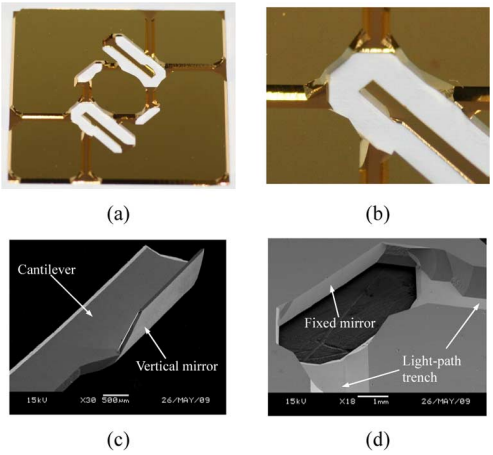

Fig. 6. (a) The pictures of the fabricated micro-mirror structure. (b) The enlarged view of the movable mirror and the cantilever. (c) The SEM photo of the movable mirror and the cantilever. (d) The SEM photo of the fixed mirror and light-path trenches.

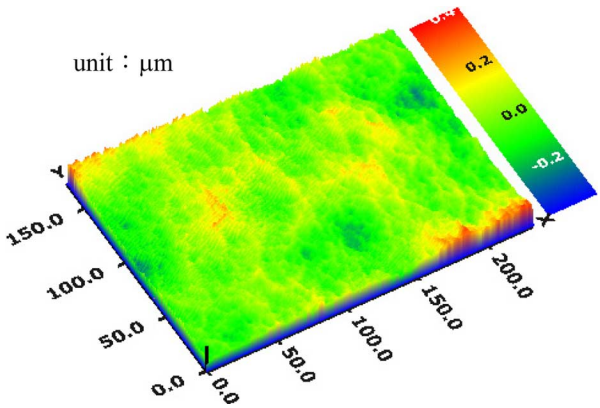

Fig. 7. The measured surface profile of the mirror. The average roughness of the mirror is 62.0 nm. The root-mean-square roughness of the mirror is 79.1 nm.

Furthermore, when compared with the *cross-bar design*, single-sided mirrors, rather than double-sided mirrors, are required for this SCB design. Therefore, the SCB design does not require complex processes for fabricating thin but large mirrors. When compared with the *mirror-array design*, the SCB design requires less movable mirrors, and thus possibly gives higher fabrication yield.

The electromagnetic bistable actuator, which is used for actuating the movable mirrors, is shown in Fig. 2(a). The picture of

TABLE I
DIMENSIONS OF THE MICROMACHINED MIRROR ARRAY

Micromachined Structures	Dimension (mm)	
Mirror plate	Width	2.1
	Height	0.72
	Thickness	0.11
Cantilever	Length	9.8
	Width	1.1
	Thickness	0.087

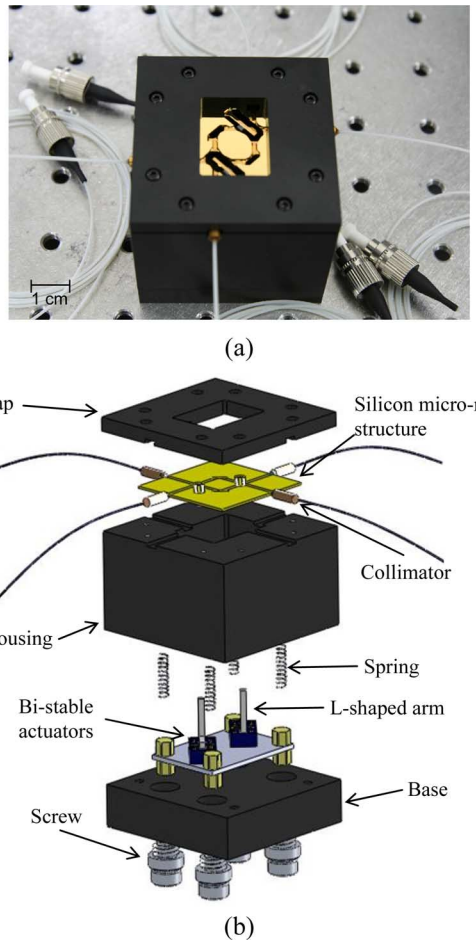

Fig. 8. (a) The prototype of the assembled SCB switch. (b) The exploded view of the switch.

the mini-actuator with an L-shaped arm is shown in Fig. 2(b). The arm is manufactured by wire-cut electrical discharge machining. The length of the arm is 10.2 mm, and the cross section is 2 mm × 2 mm. The L-shaped arm is glued on the seesaw by using epoxy. The cross-sectional drawing of the bistable actuator is shown in Fig. 2(c). Since the permanent magnet is mounted beneath the seesaw, the seesaw can retain at either of the two stable positions due to the attraction force produced by the permanent magnet. However, the seesaw can be switched between two stable positions with a stroke of about 350 μm via the magnetic field that is induced by the electromagnetic coil when applying an electrical current. The L-shaped arm is used to contact the cantilever for pushing the mirror out of the light path. Note that the contact point is designed to be at the middle of the cantilever, so the end-displacement of the cantilever (i.e.,

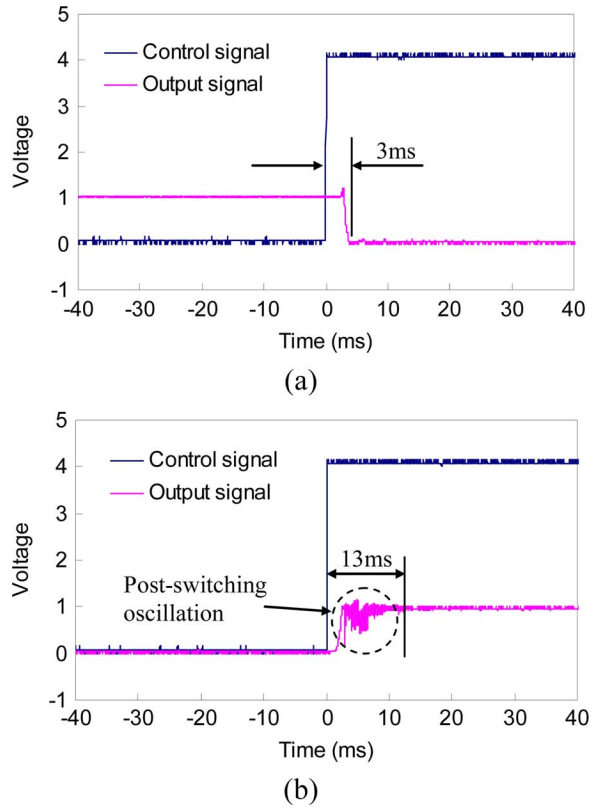

Fig. 9. The measured dynamic responses of the switch. (a) The mirror switches from the bar state to the cross state. (b) The mirror is switched from the cross state to the bar state.

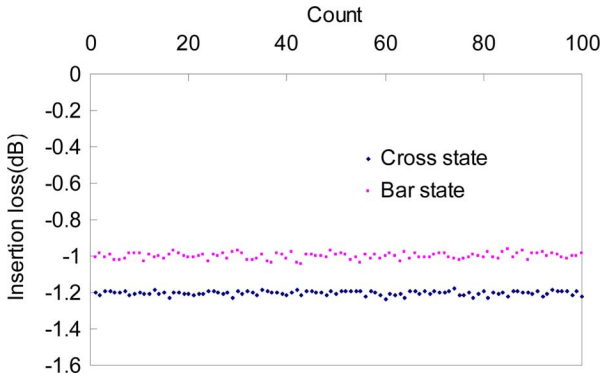

Fig. 10. The typical results of measured insertion losses for 100 switching cycles.

the displacement of the vertical mirror) is greater than the light beam width (about 500 μm).

Also, the bistable actuator is capable of holding the mirror at either one of the two stable positions without consuming any electrical power. This actuation approach not only reduces the complexity of driving circuitry, but also eliminates the concern of device temperature elevation because of the nominal power consumption of the bistable mini-actuators.

III. Mirror Array Fabrication Process

The micro-mirror structure, which includes movable mirrors, fixed mirrors, cantilevers, and light-path trenches, are realized by etching a (100) silicon wafer. The front-side mask layout of the SCB design is shown in Fig. 3(a), and the corresponding

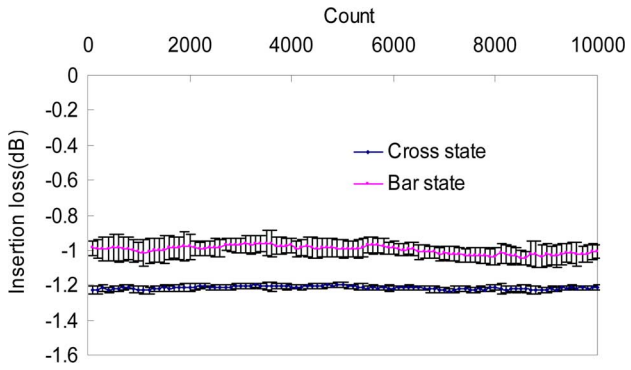

Fig. 11. The measured long-term-reliability results for 10 000 switching cycles. Each point on the curve is the average of 100 measured switching cycles.

back-side mask layout is shown in Fig. 3(b). The proposed fabrication process, which is a single-step anisotropic silicon etching process with KOH etchant, is illustrated in Fig. 4. Fig. 5 shows the simulated results by the Etch3D® with the mask patterns shown in Fig. 3. Note that the process flow in Fig. 4 is viewed on the cross section of line AA′ in Fig. 5.

The process is briefly described as follows: a double-side polished (100) silicon wafer with thickness of 800 μm is used as the starting material. Then, silicon nitride layers, which will be used as the etching masks for the micro-mirror structure, are deposited on both sides of the wafer by using low pressure chemical vapor deposition (LPCVD) (Step (i)). After patterning the nitride layers (Step (ii)), the wafer is immersed in KOH etchant (Step (iii) and Step (iv)). Vertical mirrors are formed on (100) plane during this KOH etching process under the conditions of high KOH concentration (55 wt%) and high etching temperature (75°C) [20]. Note that insufficient KOH concentration or temperature will result in inclined sidewalls. Furthermore, KOH solution added with isopropyl alcohol (IPA) can reduce the roughness of the etched surface. The residual nitride layers are removed by using phosphoric acid (Step (v)) after the micro-mirror structure is formed by the KOH etching. Then, a thin gold layer of about 2000 Å is deposited on the wafer (Step (vi)) for improving the optical reflectivity of the mirrors.

For the proposed KOH etching process, precise alignment of mask patterns to the $\langle 110 \rangle$ crystal orientation on a (100) silicon wafer is critical. Several alignment methods were reported [21], [22]. In this work, before Step (ii), a series of small circular openings are firstly patterned on the nitride layer on *the back-side of the wafer*. Then, the wafer is etched by KOH etchant for a sufficient time to form inverted pyramidal cavities. By using an optical microscope, the etched cavity, whose orientation is closest to the $\langle 110 \rangle$ direction, can be determined. This cavity will be used as the alignment mark for the subsequent mask patterns of the cantilevers and the fixed mirrors (Figs. 3(a) and (b)) [21] by using a double-side mask aligner. Furthermore, as shown in Fig. 3(a), the mask patterns of the mirrors and the light-path trenches are aligned with the $\langle 100 \rangle$ direction and the $\langle 110 \rangle$ direction, respectively. Since the angle between $\langle 100 \rangle$ and $\langle 110 \rangle$ crystallographic directions is 45°, the surfaces of the KOH-etched mirrors, which are formed on $\{100\}$ planes, will be self-aligned with the light-path trench, which is along the $\langle 110 \rangle$ direction. Therefore, the complexity of the fiber alignment procedure can be potentially reduced.

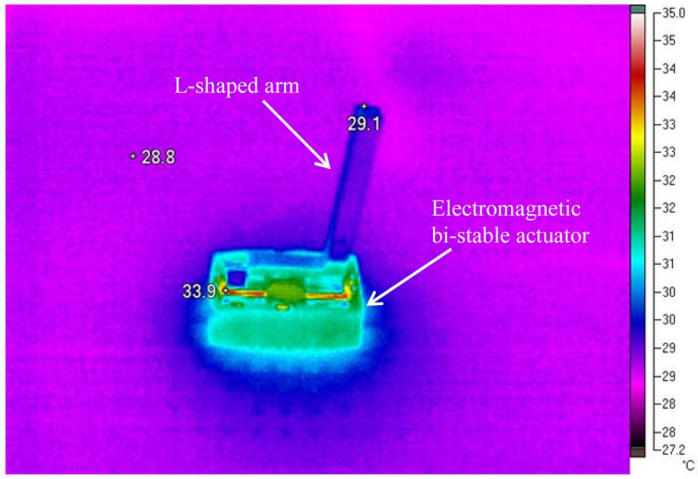

Fig. 12. The measured temperature distribution of the mini-actuator when it is working at the frequency of 50 Hz.

IV. System Assembly and Measurement

Fig. 6(a) shows the fabricated micro-mirror structure. The enlarged view of the movable mirror is shown in Fig. 6(b). Fig. 6(c) shows the SEM picture of a fabricated cantilever with a movable mirror. The SEM picture of a fixed mirror and light-path trenches is shown in Fig. 6(d). The dimensions of the components are listed in Table I. The surface profiles of the fabricated mirrors are measured by a white light interferometer. The typical surface profile measured at the center of the mirror (in a region of 230 μm $\times$ 170 μm) is shown in Fig. 7. The averaged roughness and the root-mean-square roughness of the mirror are 62.0 nm and 79.1 nm, respectively.

The picture of the SCB switch after the assembly is shown in Fig. 8(a). The exploded view of the system is shown Fig. 8(b). The micromachined silicon micro-mirror structure is mounted on the aluminum housing. The actuator module, on which two mini-actuators are soldered, is placed above the base with four pre-stressed springs. The distance between the L-shaped arms and the micro-mirror structure can be adjusted by the screws (see Fig. 8). Also, four collimators (single mode single fiber collimator, working distance: 165 mm, Photop Inc.) are aligned and glued on the grooves of the housing. For optical alignment, six axis micro stages are employed for adjusting the orientations of collimators. An IR card is used for preliminary alignment, and a power meter is used for fine alignment [23]. During the fine alignment step, once the minimum insertion loss measured by the power meter is achieved, UV glue is dispensed to immobilize the collimators.

The mini-actuators are driven by a microcontroller circuit. The mirrors can be switched between the bar-state and the cross-state with an input voltage of 5 V. The operating power is about 200 mW when switching the mirrors between two stable positions. The measured displacement of the mirror is about 630 μm, which is sufficient for the light beam to completely pass under the mirror.

Fig. 9 shows the typical dynamic response of the SCB switch. This transient result is measured by photo-diodes. When the mirror switches from the bar-state to the cross-state, the switching time is about 3 ms, as shown in Fig. 9(a). Besides, when the mirror switches from the cross-state to the bar-state, the switching time is about 13 ms, as shown in Fig. 9(b). The measured post-switching oscillation signal shown in Fig. 9(b) arises from the free-vibration of the cantilever after switching to the bar-state at which the mirror reflects light beam. This oscillation decays quickly in air (less than 13 ms), so the measured switching time meets the Bellcore requirements (less than 20 ms) [24]. Fig. 10 shows the measured insertion losses for 100 switching cycles. The average of measured insertion losses for the bar-state and the cross-state are -1 dB and -1.2 dB, respectively. The losses may be caused by the surface roughness of the mirror and the misalignment of the collimators. The measured cross-talk between each channel is about -60 dB, which can be considered negligible. The long-term reliability test of the SCB switch is performed by continuously actuating the SCB switch for 10 000 switching cycles. The measured results of the bar-state and the cross-state are plotted in Fig. 11. Each data point in Fig. 11 is the average of 100 measured data. The error bars in Fig. 11 indicate a 95% confidence interval (a span of four standard deviations). Besides, the deviations of the measured insertion losses for the cross-state and the bar-state are less than 0.05 dB after 10 000 switching cycles. Note that the optical performance of the switch is measured at the wavelength of 1550 nm.

Fig. 12 shows the measured temperature distribution of the electromagnetic mini-actuator operated at 50 Hz by using the infrared thermal imager (Fluke Inc.). Note that 50 Hz is considered as a relatively high frequency when compared with normal operations of optical switches. The temperature elevation of the pushing arm is only about 0.3°C. This tiny temperature elevation should not affect the optical performance.

V. Conclusion

A 2×2 split cross-bar (SCB) optical switch, which comprises a micromachined silicon micro-mirror structure and mini-actuators, is presented in this work. The proposed switch possesses the advantages of low actuation voltage, low cost,

low power consumption, and easy fiber alignment. The silicon micro-mirror structure can be realized monolithically by using a novel single-step anisotropic silicon etching process. Commercially-available electromagnetic bistable actuators are used to actuate the micro-mirrors. The average of measured insertion losses are -1.0 dB for the bar-state and -1.2 dB for the cross-state. Also, the measured cross-talk is about -60 dB. The measured bar-cross and cross-bar switching times are 3 ms and 13 ms, respectively. The long-term reliability test of the SCB switch is performed by continuously actuating the device for 10 000 cycles. The deviation of the measured insertion loss is less than 0.05 dB.

REFERENCES

[1] M. C. Wu, A. Solgaard, and J. E. Ford, "Optical MEMS for lightwave communication," *J. Lightw. Technol.*, vol. 24, no. 12, pp. 4433–4454, Dec. 2006.

[2] D. J. Bishop, C. R. Giles, and G. P. Austin, "The lucent LambdaRouter: MEMS technology of the future here today," *IEEE Commun. Mag.*, vol. 40, pp. 75–79, 2002.

[3] Q. H. Chen, W. G. Wu, G. Z. Yan, Z. Q. Wang, and Y. L. Hao, "Novel multifunctional device for optical power splitting, switching, and attenuating," *IEEE Photon. Technol. Lett.*, vol. 20, no. 5, pp. 632–634, Mar./Apr. 2008.

[4] R. Guerre, C. Hibert, Y. Burri, P. Fluckiger, and P. Renaud, "Fabrication of vertical digital silicon optical micromirrors on suspended electrode for guided-wave optical switching applications," *Sens. Actuators A-Phys.*, vol. 123–124, pp. 570–583, 2005.

[5] C. Marxer, C. Thio, M. A. Gretillat, N. F. deRooij, R. Battig, O. Anthamatten, B. Valk, and P. Vogel, "Vertical mirrors fabricated by deep reactive ion etching for fiber-optic switching applications," *J. Microelectromech. Syst.*, vol. 6, pp. 277–285, 1997.

[6] M. A. Basha, N. Dechev, S. Safavi-Naeini, and S. K. Chaudhuri, "A scalable $1 \times \mathrm{N}$ optical MEMS switch architecture utilizing a microassembled rotating micromirror," *IEEE J. Sel. Top. Quantum Electron.*, vol. 13, no. 2, pp. 336–347, Mar./Apr. 2007.

[7] J. J. Bernstein, W. P. Taylor, J. D. Brazzle, C. J. Corcoran, G. Kirkos, J. E. Odhner, A. Pareek, M. Waelti, and M. Zai, "Electromagnetically actuated mirror arrays for use in 3-D optical switching applications," *J. Microelectromech. Syst.*, vol. 13, pp. 526–535, 2004.

[8] D. T. Neilson, R. Frahm, P. Kolodner, C. A. Bolle, R. Ryf, J. Kim, A. R. Papazian, C. J. Nuzman, A. Gasparyan, N. R. Basavanhally, V. A. Aksyuk, and J. V. Gates, "256×256 port optical cross-connect subsystem," *J. Lightw. Technol.*, vol. 22, no. 6, pp. 1499–1509, Jun. 2004.

[9] V. A. Aksyuk, F. Pardo, D. Carr, D. Greywall, H. B. Chan, M. E. Simon, A. Gasparyan, H. Shea, V. Lifton, C. Bolle, S. Arney, R. Frahm, M. Paczkowski, M. Haueis, R. Ryf, D. T. Neilson, J. Kim, C. R. Giles, and D. Bishop, "Beam-steering micromirrors for large optical cross-connects," *J. Lightw. Technol.*, vol. 21, no. 3, pp. 634–642, Mar. 2003.

[10] X. Z. Zheng, V. Kaman, S. F. Yuan, Y. J. Xu, O. Jerphagnon, A. Keating, R. C. Anderson, H. N. Poulsen, B. Liu, J. R. Sechrist, C. Pusarla, R. Helkey, D. J. Blumenthal, and J. E. Bowers, "Three-dimensional MEMS photonic cross-connect switch design and performance," *IEEE J. Sel. Top. Quantum Electron.*, vol. 9, no. 2, pp. 571–578, Mar./Apr. 2003.

[11] H. Maekoba, P. Helin, G. Reyne, T. Bourouina, and H. Fujita, "Self-aligned vertical mirror and V-grooves applied to an optical-switch: Modeling and optimization of bistable operation by electromagnetic actuation," *Sens. Actuators A-Phys.*, vol. 87, pp. 172–178, 2001.

[12] J. Li, Q. X. Zhang, and A. Q. Liu, "Advanced fiber optical switches using deep RIE (DRIE) fabrication," *Sens. Actuators A-Phys.*, vol. 102, pp. 286–295, 2003.

[13] C. H. Ji, Y. Yee, J. Choi, S. H. Kim, and J. U. Bu, "Electromagnetic 2×2 MEMS optical switch," *IEEE J. Sel. Topics Quantum Electron.*, vol. 10, no. 3, pp. 545–550, May/Jun. 2004.

[14] D. M. Sun, W. Dong, G. D. Wang, C. X. Liu, X. Yan, B. K. Xu, and W. Y. Chen, "Study of a 2×2 MOEMS optical switch with electrostatic actuating," *Sens. Actuators A-Phys.*, vol. 120, pp. 249–256, 2005.

[15] Z. L. Huang and J. Shen, "Latching micromagnetic optical switch," *J. Microelectromech. Syst.*, vol. 15, pp. 16–23, 2006.

[16] H. Toshiyoshi and H. Fujita, "Electrostatic micro torsion mirrors for an optical switch matrix," *J. Microelectromech. Syst.*, vol. 5, pp. 231–237, 1996.

[17] G. Zhu and G.-S. Kuo, "A novel integrated multistage 2-D MEMS optical switch with spanke-benes architecture," *J. Lightw. Technol.*, vol. 26, no. 5, pp. 560–568, May 2008.

[18] Y.-J. Yang, B.-T. Liao, and W.-C. Kuo, "A novel 2×2 MEMS optical switch using the split cross-bar design," *J. Micromech. Microeng.*, vol. 17, pp. 875–882, 2007.

[19] S.-H. Chen, K.-C. Fan, T.-T. Chung, and Y.-J. Yang, "A $\mathrm{N} \times \mathrm{N}$ architecture for 2-D mirror-type optical switches," *J. Lightw. Technol.*, vol. 27, no. 14, pp. 2843–2851, Jul. 2009.

[20] O. Powell and H. B. Harrison, "Anisotropic etching of $\{100\}$ and $\{110\}$ planes in (100) silicon," *J. Micromech. Microeng.*, vol. 11, pp. 217–220, 2001.

[21] G. Ensell, "Alignment of mask patterns to crystal orientation," *Sens. Actuators A-Phys.*, vol. 53, pp. 345–348, 1996.

[22] J. M. Lai, W. H. Chieng, and Y. C. Huang, "Precision alignment of mask etching with respect to crystal orientation," *J. Micromech. Microeng.*, vol. 8, pp. 327–329, 1998.

[23] K.-C. Fan, W.-L. Lin, L.-H. Chiang, S.-H. Chen, T.-T. Chung, and Y.-J. Yang, "A 2×2 mechanical optical switch with a thin MEMS mirror," *J. Lightw. Technol.*, vol. 27, no. 9, pp. 1155–1161, May 2009.

[24] *Technical Reference TR-NWT-001073: Generic Requirements for Fiber Optic Switches,* Jan. 1994.

Bo-Ting Liao received the Ph.D. degree in mechanical engineering at National Taiwan University, Taipei, Taiwan, in 2009. He also received the M.S. degree from the Institute of Applied Mechanics, National Taiwan University, Taipei, Taiwan, in 2004; the B.S. degree in mechanical engineering at National Cheng Kung University, Tainan, Taiwan, in 2002.

His research interests include optical switch, optical MEMS, and MEMS design.

Bonnie Tingting Chia received the B.S. degree in mechanical engineering at National Taiwan University, Taipei, Taiwan, in 2006. She is now pursuing the Ph.D. degree in mechanical engineering at National Taiwan University, Taipei, Taiwan.

Her research interests include micromechanical systems, micromachining technology, and microfluidic system for biomedical applications.

Sun-Chih Shih received the B.S. and M.S. degrees in mechanical engineering at National Taiwan University, Taipei, Taiwan, in 2006 and 2008, respectively.

His research interests include optical switch, optical MEMS, and MEMS design.

Kuang-Chao Fan was born in Taiwan, on January 4, 1950. He received the B.S. degree from National Taiwan University (NTU), Taipei, in 1972, the M.S. degree from the State University of New York at Buffalo in 1976, and the Ph.D. degree from the University of Manchester Institute of Science and Technology, U.K. in 1984, all in mechanical engineering.

He has been a Professor of Mechanical Engineering with NTU since August 1989. He was promoted to the Distinguished and Chair Professor of NTU in 2007. His research interests include manufacturing metrology, precision machining, and machine tool technology. He has published around 100 journal papers and 200 conference papers. Recent topics include microcoordinate measuring machine, optical focus probe, optical switches, machine tool accuracy, and tactile sensors.

Dr. Fan received the distinguished research award from the National Science Council of ROC in 2003 and 2009.

Yao-Joe Joseph Yang received the M.S. and Ph.D. degrees in electrical engineering from Massachusetts Institute of Technology (MIT) in 1997 and 1999, respectively. Also, he received his M.S. degree (1995) from UCLA and his B.S. degree (1990) from National Taiwan University, both in mechanical engineering.

From 1999 to 2000, he joined the Coventor Inc. (Cambridge, MA) as a senior application engineer. Since 2000, he joined the Department of Mechanical Engineering at the National Taiwan University, Taipei, Taiwan. Currently he is a professor, and serves as the associate chair of the department. He is also the director for CAD Technology in the NTU NEMS Center. From 2005 to 2009, he serves as the deputy Secretary General of the Chinese Institute of Automation Engineering (CIAE). Currently he is the board member of the institute. His research interests include microelectromechanical systems, nanotechnology, high-precision micromachining, flexible sensing arrays, sensor network, parallel processing, and semiconductor devices and vacuum microelectronics modeling. He has been consulted by more than three U.S-based companies and four Taiwan-based organizations.

Dr. Yang is the recipient of the Outstanding Young Researcher Award of the National Science Council.